Published in final edited form as:
Gene Expr Patterns. 2013 October ; 13(7): 271–279. doi:10.1016/j.gep.2013.05.002.

Temporal and tissue specific gene expression patterns of the zebrafish *kinesin-1* heavy chain family, *kif5s*, during development

Philip D. Campbell and **Florence L. Marlow***
Department of Developmental and Molecular Biology, Albert Einstein College of Medicine. Yeshiva University. Bronx, NY (USA)

Abstract

Homo- and heterodimers of Kif5 proteins form the motor domain of Kinesin-1, a major plus-end directed microtubule motor. Kif5s have been implicated in the intracellular transport of organelles, vesicles, proteins, and RNAs in many cell types. There are three mammalian KIF5s. KIF5A and KIF5C proteins are strictly neural in mouse whereas, KIF5B is ubiquitously expressed. Mouse knockouts indicate crucial roles for KIF5 in development and human mutations in KIF5A lead to the neurodegenerative disease Hereditary Spastic Paraplegia. However, the developmental functions and the extent to which individual *kif5* functions overlap have not been elucidated. Zebrafish possess five *kif5* genes: *kif5Aa*, *kif5Ab*, *kif5Ba*, *kif5Bb*, and *kif5C*. Here we report their tissue specific expression patterns in embryonic and larval stages. Specifically, we find that *kif5As* are strictly zygotic and exhibit neural-specific expression. In contrast, *kif5Bs* exhibit strong maternal contribution and are ubiquitously expressed. Lastly, *kif5C* exhibits weak maternal expression followed by enrichment in neural populations. In addition, *kif5s* show distinct expression domains in the larval retina.

Keywords

Microtubules; Intracellular transport; Trigeminal ganglia; Posterior lateral line ganglia; Retina; Neurons; Hindbrain; Spinal cord; Digestive tract

1. Results and Discussion

Polarized cells like oocytes and neurons rely heavily on the proper organization of their intracellular components in order to achieve their function. Subcellular localization of organelles, proteins, and RNAs is critical for functional compartmentalization in cells. Such organization can be achieved via two main mechanisms: broadly distributed cellular components experience a selective force in specific subcellular regions (*i.e.* tethering to the plasma membrane, selective degradation or stabilization etc.) or select cellular components are actively transported to specific subcellular locations. Selective transport is a common mechanism to affect cellular asymmetry that relies on a polarized array of microtubule

*Corresponding Author: F. L. Marlow (florence.marlow@einstein.yu.edu,+1718-430-4208). Department of Developmental and Molecular Biology. Albert Einstein College of Medicine. Yeshiva University. Bronx (NY, USA). 1300 Morris Park Av. 10461, Bronx.

tracks and their associated families of molecular motor proteins that travel along the microtubules(Hirokawa, 1998; Houliston and Elinson, 1991; Lafont et al., 1994; Messitt et al., 2008). The two main classes of microtubule-based molecular motors are Kinesins, composed mainly of microtubule plus-end directed motors, and Dyneins, composed mainly of microtubule minus-end directed motors(Allan, 2011; Hirokawa et al., 2009). While Dyneins rely on a complex composed of combinations of large proteins and small peptides known as the Dynactin complex to enact cargo specificity(Allan, 2011), the Kinesin superfamily of proteins (known as Kifs) is composed of around 45 different Kinesin proteins in mammals(Miki et al., 2001), each thought to have their own cargo specificity.

The Kinesin superfamily of proteins is subdivided into three branches based on the location of the motor domain: N-terminal motor domain Kifs (N-Kifs), C-terminal motor domain KIFs (C-Kifs), and middle motor domain Kifs (M-Kifs)(Miki et al., 2001). Among the N-Kifs, the best studied motors are Kif5s. Originally named Kinesin Heavy Chains (KHCs), Kif5s were the first Kinesins discovered(Vale et al., 1985). There are three mammalian KIF5s: KIF5A, KIF5B, and KIF5C. Together, these proteins form homo- and heterodimers(Kanai et al., 2000), and are also often found in a heterotetrameric protein complex together with two Kinesin Light Chains (KLCs), originally known as conventional Kinesin, but now referred to as Kinesin-1(Bloom et al., 1988; Kuznetsov et al., 1988). While these three isoforms display striking sequence similarity, their expression patterns differ, with adult murine KIF5A and KIF5C proteins expressed only in neurons and KIF5B protein expressed ubiquitously in all tissues(Kanai et al., 2000).

Kif5s have been implicated in a wide-range of transport processes including retrograde transport of vesicles from Golgi to ER(Lippincott-Schwartz et al., 1995), anterograde transport of lysosomes to the plasma membrane(Nakata and Hirokawa, 1995), pigment dispersion in melanocytes(Hara et al., 2000), and anterograde axonal transport of organelles, proteins, vesicles, and RNAs in neurons(Hirokawa et al., 2010). Mouse knockouts have been generated for all three murine *Kif5s*. *Kif5A* knockout mice die shortly after birth due to failure to inflate their lungs(Xia et al., 2003). Among *Kif5s, Kif5B* knockout phenotypes are the most severe and these mice do not survive past 11.5 days postcoitum(Tanaka et al., 1998), making the developmental function of KIF5B difficult to study. *Kif5C* knockout mice are grossly normal and display only a modest decrease in brain size and motor neuron numbers(Kanai et al., 2000). With the exception of *Kif5B,* the relatively moderate mutant phenotypes of the other *Kif5s* suggest they may have some redundant roles.

Zebrafish possess five *kif5* genes, *kif5Aa*, *kif5Ab*, *kif5Ba*, *kif5Bb*, and *kif5C*, none of which have been carefully studied to date. To investigate the temporal and tissue specific expression patterns of the five zebrafish *kif5s* during development and in adult tissues, we have performed RT-PCR and *in situ hybridization* experiments.

1.1 Kif5 structure, phylogeny, and sequence alignment

Kif5s have a conserved stereotypical structure comprised of an N-terminal globular head/motor domain connected via a neck domain to a coiled-coil rich stalk region and a C-terminal globular tail domain (Fig. 1A). The motor domain is responsible for ATP-hydrolysis and microtubule binding allowing the complex to move along microtubules. The neck is composed of two regions, a flexible neck linker (NL) thought to be involved in velocity(Kalchishkova and Bohm, 2008) and regulation of directionality, and a coiled coil (NCC) domain thought to be important for Kif5 dimerization(Grummt et al., 1998; Marx et al., 1998). The rigid stalk is composed of two coiled coil regions (CC1/2) which allow for dimerization and two flexible hinge regions (H1/2). H2 is especially important as it allows formation of the inactive folded conformation when cargo is not bound(Friedman and Vale,

1999; Hackney et al., 1992). The C-terminal tail region is known to mediate interaction with Kinesin Light Chains (KLCs) and various cargo(Jeppesen and Hoerber, 2012).

Sequence alignment of zebrafish, human and mouse Kif5s reveals significant conservation between these proteins, particularly in the motor domain, the neck, CC1/2, H2, and the N-terminal portion of the tail (Fig. 1B). Sequence divergence among zebrafish paralogs and among mouse and human orthologs is most evident in the flexible H1 region, in the middle portion of CC2, and at the C-terminal portion of the tail. H1 is thought to allow flexibility of Kif5 dimers as they move cargo(Gutierrez-Medina et al., 2009), and so the secondary structure of these regions would be expected to be more conserved rather than the primary structure. Predictions of coiled-coil probability for the zebrafish Kif5s (zKif5s) were made using the freely available Paircoil2 program(McDonnell et al., 2006). This program predicts coiled coil domains based on amino acid sequences by using pairwise residue correlations acquired from a coiled coil database and is thought to outperform other common prediction methods. These predictions reveal that H1 has a very low probability of coiled coils (Fig. 2), allowing for flexibility in this region. The divergent sequence noticed in the middle of CC2 correlates with a small region which has zero probability of coiled coil formation in zKif5As (Fig. 2). This region may represent an additional hinge domain that is specifically found in Kif5As. Finally, the sequence differences noted in the C-terminal portion of the tail domain may lead to variability in cargo specificity.

Phylogenetic analysis of human, mouse, and zebrafish Kif5s reveals clustering of zKif5s with their respective mouse and human orthologs (Fig. 1C). zKif5Ba and zKif5Bb are most similar to their human and mouse Kif5B orthologs with 86% sequence identity. zKif5C is 78% identical to its orthologs, while zKif5Aa is 72% identical and zKif5Ab has 66% identity with mouse and human Kif5As. Furthermore, comparing the coiled coil probability profile of zKif5Ab with all other zebrafish paralogs reveals two interesting points of divergence. The first occurs in CC1 (Fig. 2, bar) where zKif5Ab appears to have a relatively low coiled coil probability compared to the its paralogs. The second occurs in CC2 where zKif5Ab once again seems to have a low coiled coil probability and also lacks the third peak present in the other profiles (Fig. 2). Among the *kif5s* duplicated in zebrafish, zKif5Ba and zKif5Bb are closely related and cluster together as expected. Interestingly, zKif5Aa and zKif5Ab appear to be more distantly related, with zKif5Aa being more closely related to human and mouse Kif5As. zKif5Ba and zKif5Bb are 90% identical to one another whereas zKif5Aa and zKif5Ab share only 67% identity. This striking difference between zKif5Aa and zKif5Ab suggests that these two genes have diverged significantly over time and may now possess non-redundant functions.

1.2 *kif5s* show distinct expression profiles during zebrafish development and in adult tissues

To determine the temporal expression profiles of zebrafish *kif5s* during development, RT-PCR analysis was performed on zebrafish embryos and larvae ranging from early cleavage stages (2 cell) to 6 days post-fertilization (dpf) (Fig. 3A). Three of the five *kif5s*, *kif5Ba*, *kif5Bb*, and *kif5C* were detected as maternal transcripts (2 cell stage). Notably, maternal expression of *kif5Ba* appeared to be stronger than *kif5Bb* and *kif5C*. *kif5Ba* expression persisted through 6dpf whereas *kif5Bb* and *kif5C* were weak or below detectable levels in blastula and gastrula stages and became robust by 24 hours post-fertilization (hpf) (Fig. 3A). In contrast, *kif5Aa* and *kif5Ab* were strictly present as zygotic transcripts, with expression first detectable at 24hpf and 48hpf respectively, among the stages assayed. *kif5Aa* and *kif5Ab* remained abundant through larval stages through 6dpf, the last stage assayed, although *kif5Aa* appeared to be more abundant at all stages assayed.

To determine the tissue-specific distribution of *kif5* transcripts in adults, RT-PCR analysis was performed on cDNA prepared from adult organs and tissues (Fig. 3B). Two of the *kif5s*, *kif5Ba* and *kif5Bb*, were expressed in all tissues assayed. While both *kif5Ba* and *kif5Bb* tissue distributions were comparable, there appeared to be slight differences in expression levels in certain tissues. Perhaps most striking was in the intestine, where *kif5Ba* expression appears more robust than *kif5Bb*. In contrast to the ubiquitous nature of the *kif5Ba* and *kif5Bb* expression profiles, *kif5Aa*, *kif5Ab*, and *kif5C* showed more restricted expression profiles and were expressed mostly in neural (brain, spinal cord, eye) tissues. Of the three genes, *kif5Aa* appeared to be the most highly expressed in all three neural tissues. In addition, *kif5Aa and kif5C* showed minor expression in reproductive tissues (testis, ovary). This is distinct from *kif5Aa* and *kif5Ab* in medaka, a close relative of zebrafish, where *kif5Ab* was detected in neural tissues, spleen, and testes whereas *kif5Aa* was only detected in neural tissues (Kawasaki et al., 2012).

Based on these expression data, we can classify the developmental and tissue expression profiles of zebrafish *kif5s* into three broad categories. *kif5Ba* and *kif5Bb* are maternally expressed transcripts that remain steady during blastula and early gastrula stages and then appear more abundant from late gastrula through 6dpf. These two genes are also ubiquitously expressed in adulthood, though their abundance appears to vary from tissue to tissue. In contrast, *kif5Aa* and *kif5Ab* are strictly zygotically expressed with expression first apparent between bud stage and 48hpf and continuing through larval stages. These genes are significantly expressed in neural tissues and *kif5Aa* is modestly expressed in reproductive tissues. Lastly, *kif5C* exhibits a mixed expression profile. *kif5C* is maternally expressed and persists through 6dpf, but is restricted to neural and reproductive tissues in adulthood.

These distinct temporal and tissue distribution profiles suggest non-overlapping function in the early zebrafish embryo as well as the adult zebrafish. Specifically, robust expression of *kif5Bs* suggests these *kif5s* contribute uniquely, along with *kif5C*, to maternally regulated processes during embryonic development and in non-neuronal and non-reproductive adult tissues; however, they could have overlapping or redundant functions with one another. In addition, overlapping expression profiles of *kif5s* in later developmental stages and/or neural and reproductive adult tissues indicate they could have both redundant and non-redundant roles. To better assess potential overlapping and redundant functions, we performed *in situ* hybridization to examine the spatial distribution of *kif5s* during embryonic and larval developmental stages.

1.3 Ubiquitous expression of *kif5Ba*, *kif5Bb*, and *kif5C* but not *kif5Aa* or *kif5Ab* during cleavage stages, gastrulation, and somitogenesis

To investigate the spatial expression patterns of zebrafish *kif5s*, whole mount *in situ* hybridization experiments were performed on embryos, pharyngula, and larvae. *kif5Aa* was found to be expressed in adult ovary; however, it was not found to be maternally expressed indicating it may be expressed in somatic tissues of the gonad rather than in the germline (Fig. 3, Fig. 4A and not shown). Because Kif5B knockout mice are early embryonic lethal(Tanaka et al., 1998) and our RT-PCR results indicate that zebrafish *kif5Ba*, *kif5Bb*, and *kif5C* are maternally expressed, we investigated whether these genes exhibited specific expression patterns during early embryogenesis. *kif5Ba*, *kif5Bb*, and *kif5C* were maternally expressed (Fig. 4B–D) and remained ubiquitously expressed in the cells of blastula (Fig. 4F–H), gastrula (Fig. 4J–L), and bud stage embryos (Fig. 4N–P). Consistent with the RT-PCR experiments, *kif5Ba* expression appeared to be more abundant than *kif5Bb* and *kif5C* during these stages. Though *kif5C* was found to have restricted expression domains in adulthood, this ubiquitous expression during early embryogenesis is in line with previous reports of *kif5C* expression in chick gastrula(V. Dathe, 2004). Ubiquitous expression of *kif5Ba*, *kif5Bb*, and *kif5C* continued during somitogenesis (Fig. 4R–T, V–X). Additionally, all three

transcripts were enriched in the trigeminal ganglion and *kif5Ba* and *kif5Bb* showed enrichment in the otic placode. Interestingly, compared to *kif5Ba* and *kif5C*, *kif5Bb* appeared to be slightly more enriched in the spinal cord as opposed to somites (Fig. 4V–X).

kif5Aa was not detected until somitogenesis (Fig.4A, E, I, M, Q, U) when it began to be expressed in the trigeminal ganglion and the spinal cord. *kif5Ab* was not detected at the blastula, gastrula, and segmentation stages assayed.

1.4 Two distinct expression patterns for zebrafish *kif5s* during embryonic, pharyngula, and larval stages

Extensive morphogenesis and tissue-specification continue after the completion of gastrulation. Our temporal analysis of *kif5* expression profiles indicated that all were expressed by the late embryo. To assess whether individual *kif5s* show distinct tissue specific expression patterns during zebrafish development which might reveal potential overlapping and non-overlapping *kif5* functions, we performed whole mount *in situ* hybridization experiments on post-gastrulation embryonic (24hpf), pharyngula (48hpf), and larval stages (96hpf). As expected based on RT-PCR analysis, all *kif5s* were detected at the post-gastrulation stages assayed. At 24hpf *kif5s* were either broadly expressed or showed restricted expression patterns within the central nervous system and neurons. *kif5Aa*, *kif5Ab*, and *kif5C* all exhibited neuron-specific expression patterns (Fig. 5). *kif5Aa* and *kif5C* were most abundant, with expression in the areas of the telencephalon, diencephalon, epiphysis, tegmentum, hindbrain, and spinal cord (Fig. 5A,E). *kif5Ab* expression resembled that of *kif5Aa* but was only very weakly detected in the telencephalon, diencephalon and hindbrain and was not detectable in the spinal cord (Fig. 5B), indicating *kif5Aa* and *kif5Ab* may have both common and divergent functions. Similarly, though *kif5Ba* and *kif5Bb* were detected with comparable abundance in most tissues (Fig. 5C,D), as was the case during somitogenesis, *kif5Bb* appeared to be enriched in the spinal cord. These data are consistent with previous reports in mice where KIF5A and KIF5C proteins are restricted to neural populations while KIF5B protein is ubiquitously expressed(Kanai et al., 2000).

To facilitate comparison of *kif5Aa* and *kif5C* expression we examined flat mounts at 24hpf. Whereas *kif5Aa* was discretely localized to the telencephalon, diencephalon, epiphysis, tegmentum, hindbrain, and spinal cord (Fig. 5F), *kif5C* had less defined expression domains and was more broadly expressed at low abundance, including expression in the eye (Fig. 5G). This may reflect persistence of the initial ubiquitous maternal expression (Fig. 4) combined with the zygotic neuron-specific expression of *kif5C*. Consistent with this notion, previous reports have shown that *kif5C* is expressed in mesodermal tissue of the early chick embryo and then later is strictly expressed in neural tissues(V. Dathe, 2004). *kif5Aa* expression was robust in the trigeminal (TGg) and the posterior lateral line (PLLg) ganglia (Fig. 5F,H), sites of cell bodies responsible for projecting relatively long axons in zebrafish(Raible and Kruse, 2000). In contrast, *kif5C* was only weakly expressed in the TGg and was not observed in the PLLg (Fig. 5G,I). Given the important role of *kif5s* in anterograde fast axonal transport of mitochondria, synaptic vesicles, proteins, and RNAs(Cai et al., 2005; Kanai et al., 2004; Su et al., 2004; Tanaka et al., 1998), as well as the known function of *kif5A* in the slow axonal transport of neurofilaments(Xia et al., 2003), expression of *kif5Aa* and *kif5C*, may be functionally important in zebrafish development.

In addition to strong expression in the central nervous system, *kif5Ba* and *kif5Bb* were also strongly expressed in somites (Fig. 5C,D). Recent reports have implicated KIF5B in the transport and organization of myofibril components and intermediate filament components in mouse myoblasts(Wang et al., 2013). Given the abundant expression of *kif5Bs* in these tissues, it is possible that they fulfill similar functions in zebrafish.

During pharyngula (48hpf) and larval (96hpf) stages, the *kif5s* continued to show either CNS and neural, *kif5Aa*, *kif5Ab*, and *kif5C*, or ubiquitous, *kif5Ba* and *kif5Bb,* patterns of expression. The three neural *kif5s* were all present in the spinal cord, though *kif5Aa* expression appeared to be most abundant (Fig. 6A–D,I,J). Of particular interest was the high expression of *kif5As* in the developing nose (Fig. 6A–D). Although Kinesin-2 plays a role in transporting cyclic nucleotide-gated channels in olfactory sensory neurons(Jenkins et al., 2006), little is known about the roles of Kinesins in olfactory neurons. While the two *kif5Bs* remained ubiquitously expressed, *kif5Bb* continued to become weaker in the somites or was more enriched in the spinal cord (Fig. 6E–H). In addition to this pattern, *kif5Ba* and *kif5Bb* expression became robust in the developing digestive tract at larval stages (Fig. 5F,H). At this stage *kif5Ba* appeared to be more abundant, consistent with the RT-PCR results of adult intestine (Fig. 3B).

1.5 *kif5s* are differentially expressed in the zebrafish retina

All five of the zebrafish *kif5s* were found to be expressed in the larval retina, however, little is known about the role of *kif5s* in this tissue. To assess the expression pattern of *kif5s* in the zebrafish larval retina, eyes were removed from 96hpf whole mount *in situ* larvae so that the retinal layers could be visualized. As was the case in other experiments, both *kif5Ba* and *kif5Bb* were the most broadly expressed and were detected at variable degrees throughout all layers of the retina (Fig. 7C,D,G). In contrast, *kif5Aa*, *kif5Ab*, and *kif5C* were not detected in the outer nuclear layer (ONL), but were detected throughout the rest of the retina. Of particular interest, *kif5Ab* was only present in the inner portion of the inner nuclear layer (INL), where the majority of amacrine cells are located(Connaughton et al., 2004). All of the *kif5s*, except for *kif5Ab* displayed robust expression in the inner plexiform layer (IPL), with *kif5Aa*, *kif5Ba*, and *kif5Bb* appearing most robust in the ganglion cell layer (GCL). While we cannot exclude that differences in tissue thickness may limit detection of transcripts in the outer layer, these findings are distinct from immunofluorescence experiments of adult bovine and human retinas that showed KIF5A/C protein restricted to the ONL and optic nerve fiber layer (ONFL) and Kif5B protein in all layers except for the ONL(Mavlyutov et al., 2002).

Our results suggest that zebrafish *kif5s* play important roles during development. While a subset of *kif5s* displayed overlapping expression domains at particular developmental time points, others displayed distinct expression patterns, suggesting both redundant and specific *kif5* functions during development. Future overexpression and knockdown studies of zebrafish *kif5s* will delineate these functions.

2. Experimental procedures

2.1 Animals

AB strain zebrafish embryos were generated by natural pairwise matings. They were staged and reared according to standard procedures(Wester eld, 1995). Embryos and larvae were fixed in 4% paraformaldehyde. The stages analyzed were cleavage (32 cell), blastula (sphere), gastrula (shield, bud), somitogenesis (15, 19 somtes), pharyngula (24, 36, 48 hpf), and larva (3, 4, 5, 6 dpf).

All procedures and experimental protocols were in accordance with NIH guidelines and approved by the Einstein IACUC under protocol #20110714.

2.2 Phylogram, Protein Alignment, and Coiled coil Prediction

FASTA protein sequences corresponding to the longest known alternative transcript (around 1kb) for each of the zebrafish, mouse, and human *kif5s* were obtained from the Ensembl

website (www.ensembl.org) and analyzed using the Satchmo online software provided by the University of Berkeley (http://phylogenomics.berkeley.edu/q/satchmo/)(Hagopian et al., 2010). The phylogram and protein alignment were visualized and the figures were created using the free open-source bioinformatics software Unipro UGENE v1.11 (http://ugene.unipro.ru/). Predictions of the paired coiled-coil fold from Kif5 protein sequences were made using the Paircoil2 software(McDonnell et al., 2006). Ensembl ID numbers are as follows:

zKif5Aa: ENSDART00000110704; zKif5Ab: ENSDART00000090634;

mKif5A: ENSMUST00000099172; hKif5A: ENST00000455537;

zKif5Ba: ENSDART00000113849; zKif5Bb: ENSDART00000084802;

mKif5B: ENSMUST00000025083; hKif5B: ENST00000302418;

zKif5C: ENSDART00000083567; mKif5C: ENSMUST00000028102;

hKif5C: ENST00000435030.

2.3 RT-PCR

Total RNA was extracted from the specified developmental stages and adult tissues using Trizol Reagent (Invitrogen). For developmental stages, 30 embryos or larvae were collected for each sample. For adult tissues, 1–6 organs harvested from adult zebrafish were pooled. cDNA synthesis was performed using SuperScript III First-Strand Synthesis System (Invitrogen) according to manufacturer instructions. No RT (NRT) control samples were prepared by omitting reverse transcriptase from the cDNA synthesis.

The concentration of cDNA was determined by measuring the absorbance at 260 nm using a Nanodrop ND-1000 Spectrophotometer, and 0.25 ug was used for each reaction. PCR reactions were performed using Taq Polymerase. The following primers were used:

kif5Aa 5′GAGCAGTCCAAACAGGATCTCA3′,

5′ACAGCGGAGATCTGCATTATCA3′

kif5Ab 5′AGGAGCAGAAACCCCTTCAG3′

5′TCTTTCGTGCTTGAAAGTGTC3′

kif5Ba 5′GACTTTGCACAACCTCAGGAAA3′,

5′GCAGACGCTTCTCCAGTTTAGG3′,

kif5Bb 5′TCTCAATGAGGAGCTGGTCAAA3′,

5′GTTTTTCATGCTCCACCTTCAA3′

kif5C 5′AGCGGGATCTATCATCCTTGAA3′,

5′TCTGCGTGCTCTCTAGCTGTTT3′

ef1a 5′AGCCTGGTATGGTTGTGACCTTCG3′,

5′CCAAGTTGTTTTCCTTTCCTGCG3′

PCR reactions were performed using an Eppendorf Mastercycler and the following conditions: 95°C for 2 min followed by 30 cycles of 95°C for 20 s, 57°C for 20 s, and 72°C for 30 s and a final extension of 72°C for 10 min.

2.4 In situ hybridization

In situ hybridization was performed according to established protocols(Thisse and Thisse, 2008). To make *in situ* probes, C-terminal fragments of *kif5Aa, kif5Ab, kif5Ba, kif5Bb,* and *kif5C* were amplified from 5 dpf cDNA and cloned into pGEMT (Promega) for *kif5Aa*, *kif5Ab*, *kif5Ba*, and *kif5Bb* or pSC-A (Agilent) for *kif5C*. Probes were amplified based on sequences from the Sanger Ensembl ZV9 Genome with the following gene identification numbers:

kif5Aa: ENSDARG00000005470; *kif5Ab*: ENSDARG00000059818;

kif5Ba: ENSDARG00000074131; *kif5Bb*: ENSDARG00000075251;

kif5C: ENSDARG00000076027.

The probes were designed to target the following regions: *kif5Aa* 3′ UTR; *kif5Ab* exons 20–25; *kif5Ba* exons 16–25; *kif5Bb* exons 13–25; *kif5C* exons 17–25. For antisense probes, plasmids were linearized using NotI for *kif5Aa* and *kif5C*, ApaI for *kif5Ab*, *kif5Ba*, and *kif5Bb*, and riboprobes were synthesized with T7 RNA polymerase for *kif5Aa*, Sp6 RNA polymerase for *kif5Ab*, *kif5Ba*, and *kif5Bb*, and T3 RNA polymerase for *kif5C*. For sense probes, plasmids were linearized using ApaI for *kif5Aa* and *kif5C*, NotI for *kif5Ab*, and SpeI for *kif5Ba* and *kif5Bb*, and the riboprobes were synthesized with Sp6 RNA polymerase for *kif5Aa*, T7 RNA polymerase for *kif5Ab*, *kif5Ba*, *kif5Bb*, and *kif5C*. Probes were detected using anti-DIG-AP antibody (1:5000, Roche) and colorimetric reactions were performed using BM Purple AP Precipitating Substrate (Roche). No significant staining was observed with the sense probes.

2.6 Image acquisition and analysis

Whole-mount *in situ* hybridization signals of embryos and larvae were imaged using an Olympus SZ61 dissecting microscope with a high-resolution digital camera (model S97809, Olympus America) and Picture Frame 2.0 or 3.0 software (Optronics). Flat-mount *in situ* hybridization embryos and larvae were imaged using a Zeiss Axioskop2 plus upright microscope with a Zeiss AxioCam MRc camera and Zeiss AxioVision Rel. 4.6 software. Images were processed using ImageJ and final figure adjustments were made using Adobe® Illustrator® CS6.

Acknowledgments

We thank Dr. Adrian Santos-Ledo, Dr. Lei Feng, and Xin Li for their valuable comments on the manuscript, Marlow lab members for discussion, and Spartak Kalinin and Clint Depaolo for zebrafish care. Research of the Marlow lab is funded by NIH R01GM1089979 and startup funds to F. Marlow. P. Campbell was supported in part by the Albert Einstein College of Medicine MSTP training grant T32-GM007288.

References

Allan VJ. Cytoplasmic dynein. Biochemical Society transactions. 2011; 39:1169–1178. [PubMed: 21936784]

Bloom GS, Wagner MC, Pfister KK, Brady ST. Native structure and physical properties of bovine brain kinesin and identification of the ATP-binding subunit polypeptide. Biochemistry. 1988; 27:3409–3416. [PubMed: 3134048]

Cai Q, Gerwin C, Sheng ZH. Syntabulin-mediated anterograde transport of mitochondria along neuronal processes. The Journal of cell biology. 2005; 170:959–969. [PubMed: 16157705]

Connaughton VP, Graham D, Nelson R. Identification and morphological classification of horizontal, bipolar, and amacrine cells within the zebrafish retina. The Journal of comparative neurology. 2004; 477:371–385. [PubMed: 15329887]

Friedman DS, Vale RD. Single-molecule analysis of kinesin motility reveals regulation by the cargo-binding tail domain. Nature cell biology. 1999; 1:293–297.

Grummt M, Woehlke G, Henningsen U, Fuchs S, Schleicher M, Schliwa M. Importance of a flexible hinge near the motor domain in kinesin-driven motility. The EMBO journal. 1998; 17:5536–5542. [PubMed: 9755154]

Gutierrez-Medina B, Fehr AN, Block SM. Direct measurements of kinesin torsional properties reveal flexible domains and occasional stalk reversals during stepping. Proceedings of the National Academy of Sciences of the United States of America. 2009; 106:17007–17012. [PubMed: 19805111]

Hackney DD, Levitt JD, Suhan J. Kinesin undergoes a 9 S to 6 S conformational transition. The Journal of biological chemistry. 1992; 267:8696–8701. [PubMed: 1569110]

Hagopian R, Davidson JR, Datta RS, Samad B, Jarvis GR, Sjolander K. SATCHMO-JS: a webserver for simultaneous protein multiple sequence alignment and phylogenetic tree construction. Nucleic acids research. 2010; 38:W29–34. [PubMed: 20430824]

Hara M, Yaar M, Byers HR, Goukassian D, Fine RE, Gonsalves J, Gilchrest BA. Kinesin participates in melanosomal movement along melanocyte dendrites. The Journal of investigative dermatology. 2000; 114:438–443. [PubMed: 10692101]

Hirokawa N. Kinesin and dynein superfamily proteins and the mechanism of organelle transport. Science. 1998; 279:519–526. [PubMed: 9438838]

Hirokawa N, Niwa S, Tanaka Y. Molecular motors in neurons: transport mechanisms and roles in brain function, development, and disease. Neuron. 2010; 68:610–638. [PubMed: 21092854]

Hirokawa N, Noda Y, Tanaka Y, Niwa S. Kinesin superfamily motor proteins and intracellular transport. Nature reviews. Molecular cell biology. 2009; 10:682–696. [PubMed: 19773780]

Houliston E, Elinson RP. Evidence for the involvement of microtubules, ER, and kinesin in the cortical rotation of fertilized frog eggs. The Journal of cell biology. 1991; 114:1017–1028. [PubMed: 1714912]

Jenkins PM, Hurd TW, Zhang L, McEwen DP, Brown RL, Margolis B, Verhey KJ, Martens JR. Ciliary targeting of olfactory CNG channels requires the CNGB1b subunit and the kinesin-2 motor protein, KIF17. Current biology : CB. 2006; 16:1211–1216. [PubMed: 16782012]

Jeppesen GM, Hoerber JK. The mechanical properties of kinesin-1: a holistic approach. Biochemical Society transactions. 2012; 40:438–443. [PubMed: 22435827]

Kalchishkova N, Bohm KJ. The role of Kinesin neck linker and neck in velocity regulation. Journal of molecular biology. 2008; 382:127–135. [PubMed: 18640125]

Kanai Y, Dohmae N, Hirokawa N. Kinesin transports RNA: isolation and characterization of an RNA-transporting granule. Neuron. 2004; 43:513–525. [PubMed: 15312650]

Kanai Y, Okada Y, Tanaka Y, Harada A, Terada S, Hirokawa N. KIF5C, a novel neuronal kinesin enriched in motor neurons. The Journal of neuroscience : the official journal of the Society for Neuroscience. 2000; 20:6374–6384. [PubMed: 10964943]

Kawasaki T, Kurauchi K, Higashihata A, Deguchi T, Ishikawa Y, Yamauchi M, Sasanuma M, Hori H, Tsutsumi M, Wakamatsu Y, Yuba S, Kinoshita M. Transgenic medaka fish which mimic the endogenous expression of neuronal kinesin, KIF5A. Brain research. 2012; 1480:12–21. [PubMed: 22975131]

Kuznetsov SA, Vaisberg EA, Shanina NA, Magretova NN, Chernyak VY, Gelfand VI. The quaternary structure of bovine brain kinesin. The EMBO journal. 1988; 7:353–356. [PubMed: 3130248]

Lafont F, Burkhardt JK, Simons K. Involvement of microtubule motors in basolateral and apical transport in kidney cells. Nature. 1994; 372:801–803. [PubMed: 7997271]

Lippincott-Schwartz J, Cole NB, Marotta A, Conrad PA, Bloom GS. Kinesin is the motor for microtubule-mediated Golgi-to-ER membrane traffic. The Journal of cell biology. 1995; 128:293–306. [PubMed: 7844144]

Marx A, Thormahlen M, Muller J, Sack S, Mandelkow EM, Mandelkow E. Conformations of kinesin: solution vs. crystal structures and interactions with microtubules. European biophysics journal : EBJ. 1998; 27:455–465. [PubMed: 9760727]

Mavlyutov TA, Cai Y, Ferreira PA. Identification of RanBP2- and kinesin-mediated transport pathways with restricted neuronal and subcellular localization. Traffic. 2002; 3:630–640. [PubMed: 12191015]

McDonnell AV, Jiang T, Keating AE, Berger B. Paircoil2: improved prediction of coiled coils from sequence. Bioinformatics. 2006; 22:356–358. [PubMed: 16317077]

Messitt TJ, Gagnon JA, Kreiling JA, Pratt CA, Yoon YJ, Mowry KL. Multiple kinesin motors coordinate cytoplasmic RNA transport on a subpopulation of microtubules in Xenopus oocytes. Developmental cell. 2008; 15:426–436. [PubMed: 18771961]

Miki H, Setou M, Kaneshiro K, Hirokawa N. All kinesin superfamily protein, KIF, genes in mouse and human. Proceedings of the National Academy of Sciences of the United States of America. 2001; 98:7004–7011. [PubMed: 11416179]

Nakata T, Hirokawa N. Point mutation of adenosine triphosphate-binding motif generated rigor kinesin that selectively blocks anterograde lysosome membrane transport. The Journal of cell biology. 1995; 131:1039–1053. [PubMed: 7490281]

Raible DW, Kruse GJ. Organization of the lateral line system in embryonic zebrafish. The Journal of comparative neurology. 2000; 421:189–198. [PubMed: 10813781]

Su Q, Cai Q, Gerwin C, Smith CL, Sheng ZH. Syntabulin is a microtubule-associated protein implicated in syntaxin transport in neurons. Nature cell biology. 2004; 6:941–953.

Tanaka Y, Kanai Y, Okada Y, Nonaka S, Takeda S, Harada A, Hirokawa N. Targeted disruption of mouse conventional kinesin heavy chain, kif5B, results in abnormal perinuclear clustering of mitochondria. Cell. 1998; 93:1147–1158. [PubMed: 9657148]

Thisse C, Thisse B. High-resolution in situ hybridization to whole-mount zebrafish embryos. Nature protocols. 2008; 3:59–69.

Dathe V, Brand-Saberi FPB. Expression of kinesin kif5c during chick development. Anatomy and embryology. 2004; 207:475–480. [PubMed: 14758548]

Vale RD, Reese TS, Sheetz MP. Identification of a novel force-generating protein, kinesin, involved in microtubule-based motility. Cell. 1985; 42:39–50. [PubMed: 3926325]

Wang Z, Cui J, Wong WM, Li X, Xue W, Lin R, Wang J, Wang P, Tanner JA, Cheah KS, Wu W, Huang JD. Kif5b controls the localization of myofibril components for their assembly and linkage to the myotendinous junctions. Development. 2013; 140:617–626. [PubMed: 23293293]

Wester eld, M. A Guide for the Laboratory Use of Zebra sh (Danio rerio). 1995. The Zebra sh Book.

Xia CH, Roberts EA, Her LS, Liu X, Williams DS, Cleveland DW, Goldstein LS. Abnormal neurofilament transport caused by targeted disruption of neuronal kinesin heavy chain KIF5A. The Journal of cell biology. 2003; 161:55–66. [PubMed: 12682084]

Highlights

- Zebrafish Kif5s are phylogenetically related to their mammalian orthologs
- Only *kif5Ba*, *kif5Bb*, and *kif5C* transcripts are maternally provided
- *kif5Aa*, *kif5Ab*, and *kif5C* transcripts are restricted to neural tissues of late embryos
- Ubiquitous *kif5Bs* become enriched in the larval brain and digestive tract
- *kif5s* show distinct expression domains in the zebrafish larval retina

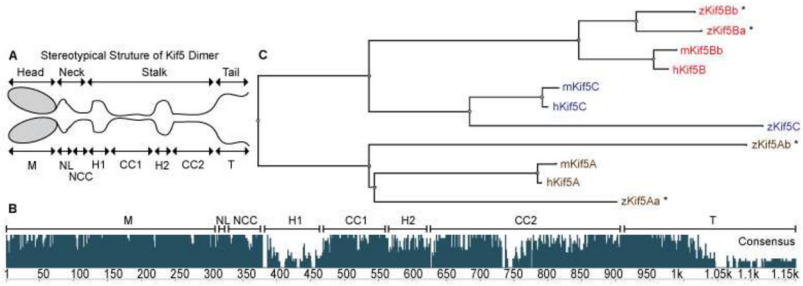

Fig. 1.

Vertebrate Kif5 protein comparison. (A) Schematic of the protein domains of a Kif5 dimer. (B) Conservation of amino acid sequence between zebrafish, mouse, and human Kif5s. (C) Phylogenetic relationship between zebrafish, mouse, and human Kif5 proteins. Orthologs are shown in the same color (Kif5A, brown; Kif5B, red; Kif5C, blue) and paralogs are denoted with an asterisk (*). The length of the branches represents the degree of change between the sequences. M, Motor domain; NL, Neck linker; NCC, Neck coiled-coil; H1, Hinge 1; CC1, Coiled-coil 1; H2, Hinge 2; CC2, Coiled-coil 2; T, Tail.

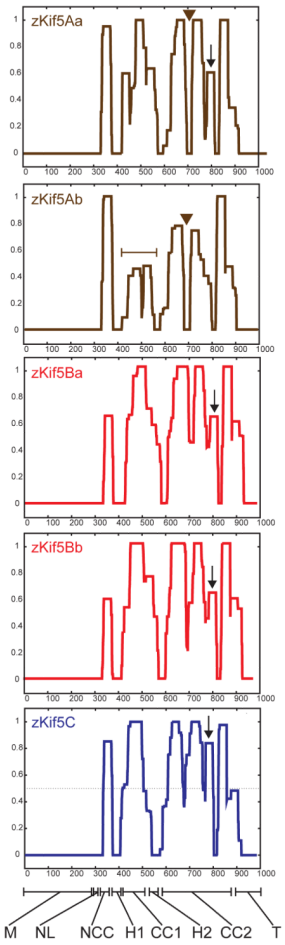

Fig. 2.

Graphs indicate the probability (y-axis) of a paired coiled coil fold occurring at a given amino acid position (x-axis) for each of the zebrafish Kif5s. Brown arrowheads denote Kif5A-specific non-coiled coil region within CC2, brown bracket denotes Kif5Ab-specific divergent region of CC1, and black arrows denote Kif5Ab-specific divergent region of CC2.

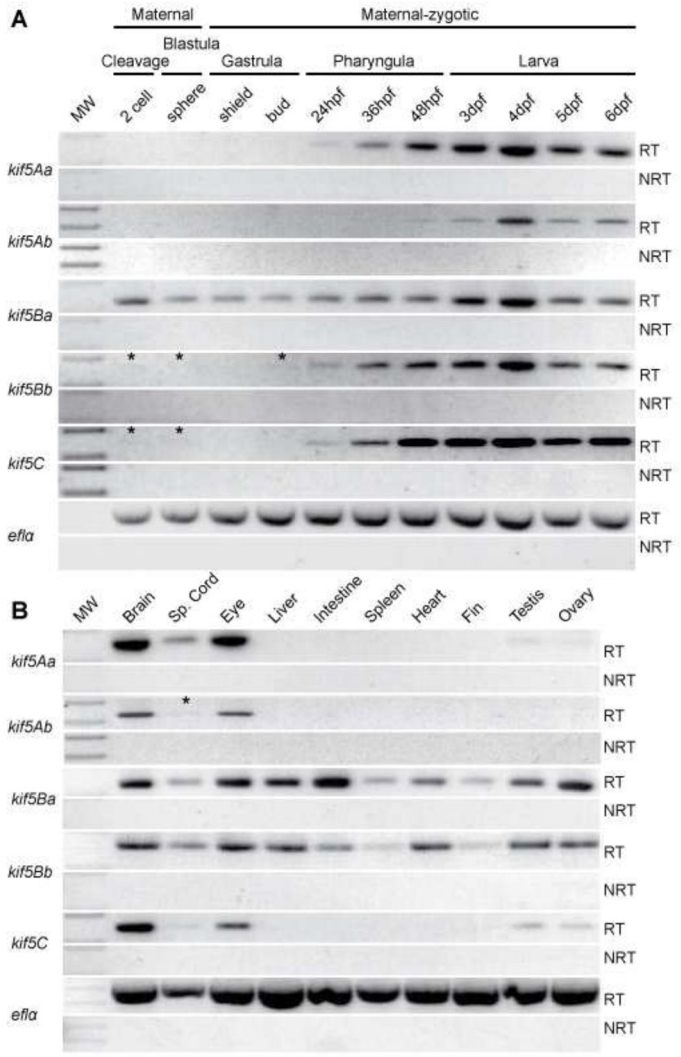

Fig. 3.

(A) Temporal analysis of zebrafish *kif5s* during development by RT-PCR. (B) RT-PCR analysis of zebrafish *kif5* tissue and organ specific expression. Asterisk (*) indicates faint bands present. NRT, no reverse transcriptase.

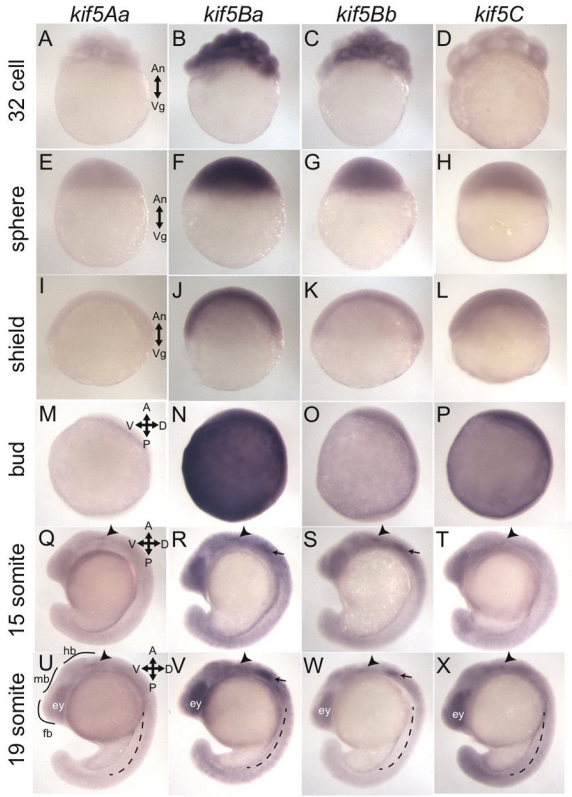

Fig. 4.

kif5 expression during early zebrafish development. Maternal expression of *kif5s* was apparent in cleavage stage for *kif5Ba*, *kif5Bb*, and *kif5C*, but not *kif5Aa* (A–D). Expression of *kif5s* at sphere (E–H), shield (I–L), bud (M–P), 15 somite (Q–T), and 19 somite (U–X) stages. Arrowheads indicate trigeminal ganglion and arrows indicate otic placode. All images are lateral views. For A–L, An=Animal pole, Vg=vegetal pole. For M–X, A=Anterior, P=Posterior, V=Ventral, D=Dorsal. Dashed line represents border between notochord and spinal cord. fb, forebrain; mb, midbrain; hb, hindbrain; ey, eye.

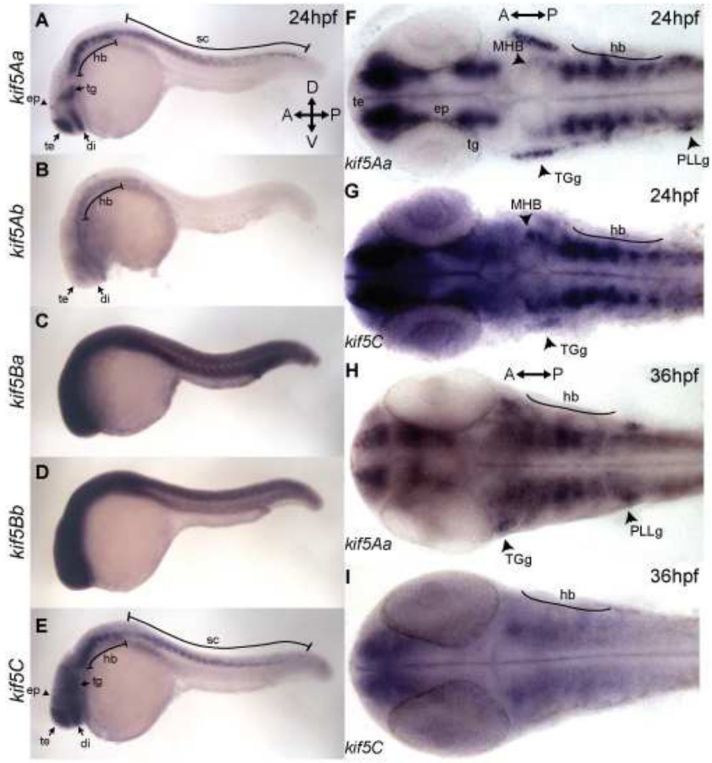

Fig. 5.

Expression of *kif5s* at 24hpf and 36hpf. (A–E) Lateral views of whole mount *in situs* at 24hpf. *kif5Aa*, *kif5Ab*, and *kif5C* were detected in the telencephalon (te), diencephalon (di), and hindbrain (hb). *kif5Aa* and *kif5C* were also detected in the tegmentum (tg), epiphysis (ep), and spinal cord (sc). *kif5Ba* and *kif5Bb* were ubiquitously expressed. (F, G) Dorsal view of flat mounts at 24hpf. *kif5Aa* and *kif5C* were detected in the midbrain-hindbrain boundary (MHB) and trigeminal ganglia (TGg). *kif5Aa* was also detected in the posterior lateral line ganglia (PLLg) while *kif5C* was more broadly expressed in other tissues. (H, I) Dorsal view of flat mounts at 36hpf. Anterior is to the left, dorsal to the top for A–E. Anterior is to the left for F–I. MHB, midbrain-hindbrain boundary.

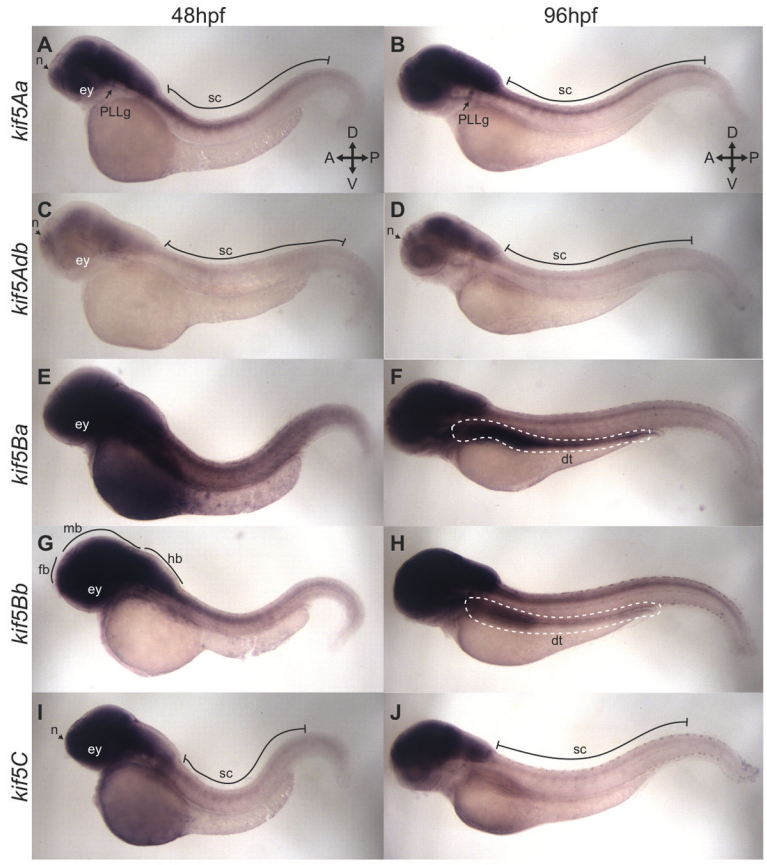

Fig. 6.

Expression of *kif5s* at 48hpf and 96hpf. (A,C,E,G,I) Lateral views of whole mount *in situs* at 48hpf. *kif5Aa*, *kif5Ab*, and *kif5C* were detected throughout the central nervous system while *kif5Bb* and *kif5Bb* were ubiquitously expressed. (B,D,F,H,J) Lateral views of whole mount *in situs* at 96hpf. *kif5Aa*, *kif5Ab*, and *kif5C* continued to be expressed in the central nervous system. *kif5Ba* and *kif5Bb* were ubiquitously expressed and showed robust expression in the digestive tract (dt). A=Anterior, P=Posterior, V=Ventral, D=Dorsal. fb, forebrain; mb, midbrain; hb, hindbrain; n, nose; ey, eye.

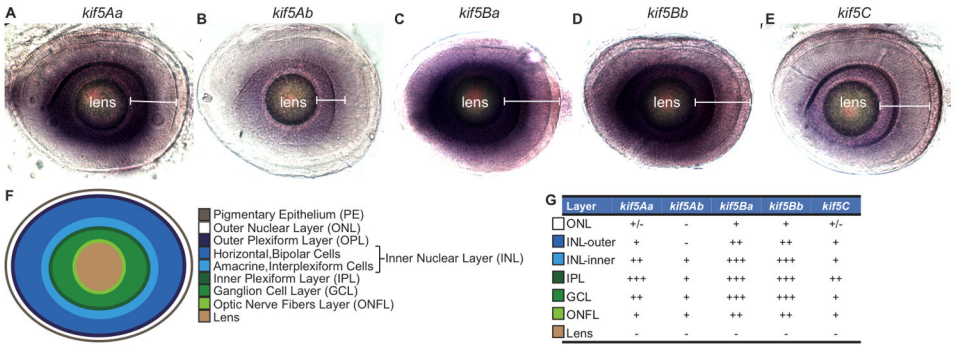

Fig. 7.

(A–E) Expression of *kif5s* in the retina at 96hpf. White brackets show the expression domain of each individual *kif5*. (F) Diagram of zebrafish retinal organization. (G) Table summarizes the relative abundance of each individual *kif5* across the retinal layers.